Evaluation of the Dynamic Yield Strength of Solids by Means of the Richtmyer-Meshkov Instability

J.J. López Cela[*,1], A.R. Piriz[*,1] and N.A. Tahir[2]

[1]*E.T.S.I. Industriales, Universidad de Castilla-La Mancha and Instituto de Investigaciones Energéticas, 13071 Ciudad Real, Spain*

[2]*Gesellschaft für Schwerionenforschung Darmstadt, Planckstrasse 1, 64291, Darmstadt, Germany*

Abstract: An experimental procedure to evaluate the dynamic yield strength of solids based on measuring the growth of the Richtmyer-Meshkov instability is proposed. To induce the Richtmyer-Meshkov instability in solids a shock is needed, so this technique is complementary to the one based on the Rayleigh-Taylor instability that is achieved by means of an isentropic compression. We have presented an analytical model elsewhere, validated against extensive finite element simulations, that describes the evolution of the Richtmyer-Meshkov instability in elastoplastic solids. The model shows that after reaching a maximum value, the time evolution of the perturbation at the solid interface remains oscillating. The maximum perturbation amplitude depends essentially on the yield strength of the material. The proposed technique needs only one experimental measurement that is related, through the scaling law given by the analytical model, to the yield strength of the material.

1. INTRODUCTION

The strength behaviour of materials under extreme conditions of pressure, strain rate and temperature is of great importance for many technological applications as well as for basic science. Amongst the first ones we can find, for instance, armor design, performance of debris for spacecraft, hypervelocity impact problems including high-velocity machining of materials [1, 2] or laser shock processing for improving fatigue and wear resistance of metals [3]. Besides, knowledge of this behaviour is of interest to understand many problems of planetary sciences as, for example, the Earth mantle convection and the modelling of planet interiors [4-7].

The origin of this problem can be found in the experimental procedure originally proposed by G. I. Taylor to determine the dynamic yield point of metals by impacting cylinders on a rigid boundary [8] and experimentally implemented by Whiffin [9]. Using a rigid plastic model of material behaviour, Taylor developed an approximate formula that related the profile of the rod after impact with the dynamic yield point of the rod. Some years later, M. L. Wilkins and M. W. Guinan treated this same problem by means of computer simulations [10]. Since then, an important effort has been done to obtain these material properties, in particular, the shear stress that a material can sustain above the Hugoniot elastic limit (HEL). The HEL or maximum stress for one-dimensional elastic wave propagation in plate geometries [11] is now easily measured using stress gauges or optical diagnostics [1]. Following this reference, the main experimental techniques for strength measurement at high pressures proposed during these years are: comparison to hydrostatic response, lateral stress gauges, pressure-shear loading, X-ray diffraction, strength measurements in diamond anvil cells, the self-consistent method and the measurement of the growth of Rayleigh-Taylor instability (RTI).

We focus our attention in the last technique, the determination of the dynamic yield strength by measuring the growth of the RTI. This method is based on the pioneering work by Barnes *et al*. [12, 13] who measured the growth of a sinusoidal perturbation in the surface of a flat plate smoothly accelerated by expanding detonation products and correlated this growth with the shear strength of the material. Nowadays, this technique is playing an increase role in the experimental evaluation of the yield strength and it has been developed by accelerating the solid by means of laser facilities [14-19]. Since the hydrodynamic instabilities in solids impose limitations in, for example, the implementation of the inertial confinement fusion and other important technological processes, an intense research activity has been developed in this field directed to understand and avoid such instabilities. However, as pointed out by Mikhailov it is possible to change the point of view and to consider the instabilities in solid media not only an object of investigation but also an investigation tool [20].

We propose an experimental technique to determine the dynamic yield strength based on other hydrodynamic instability, namely, the Richtmyer-Meshkov instability (RMI) that will occur when a shock is launched into a material sample from the free surface. For this reason we have performed extensive numerical simulations by means of the finite element method and we have also developed an analytical model that captures the main physics of the RMI in elastoplastic solids [21]. With the obtained conclusions we propose an experiment that may allow obtaining the dynamic yield strength. The two methods based on hydrodynamic

*Address correspondence to these authors at the E.T.S.I. Industriales, Universidad de Castilla-La Mancha and Instituto de Investigaciones Energéticas, 13071 Ciudad Real, Spain; E-mails: juanjose.lopez@uclm.es, Roberto.piriz@uclm.es

instabilities are complementary because they explore two different regimes. To use the RTI based technique the sample should be accelerated in an isentropic manner. Because this is, in practise, impossible a great effort is done in achieving quasi-isentropic compression [16-18]. This kind of compression allows reaching very large pressures before melting the sample but it needs the use of very big facilities due to de fact that a considerable amount of the delivery energy is used in achieve a smooth acceleration of the media. On the other hand, to use the RMI based technique, a shock is needed. In this situation, almost all of the energy delivered by the device can be transferred to the sample and, in consequence, medium-scale facilities can be employed. However, the pressure that can be achieved by a shock before melting is much lower than in an isentropic compression [22].

The paper is organized as follows: In section 2 a summary of the numerical model used in the simulations is given. Section 3 describes the shock propagation in solids when they are modelled by means of an equation of state for the volumetric part and a perfectly elastoplastic model for the deviatoric part of the stress tensor. Section 4 has two parts; in the first one, a description of the Richtmyer-Meshkov instability in solids is given while in the second one the proposed experimental technique is described. Finally, some conclusions are outlined in section 5.

2. NUMERICAL SIMULATIONS OF SOLIDS UNDER HIGH COMPRESSION

In this section we describe the numerical method we have used to perform the simulations of solids under high compression. The numerical calculations have been performed with the explicit version of the ABAQUS finite element code which is suitable for modelling fast transient phenomena [23]. The explicit version is based on a central difference scheme for the time integration of the equations of motion of the body. The algorithm has second-order accuracy and is conditionally stable. This means that the time step size is fixed according to stability requirements resulting from the Courant criteria.

To model solids under high compressions the behaviour of the material is composed of a volumetric and a deviatoric part [1]. The hydrostatic behaviour is governed by an equation of state (EOS) while the deviatoric behaviour is governed by a constitutive law, assuming that these two responses are uncoupled.

The material hydrostatic behaviour is defined by the Mie-Grüneisen equation of state as, for example, in reference [24]:

$$P - P_h = \Gamma \rho (E - E_h) \tag{1}$$

where P and E are the pressure and specific internal energy and P_h and E_h are the Hugoniot pressure and Hugoniot specific internal energy, respectively. The latter are functions of the material density ρ only. Also Γ is the Grüneisen rate defined as:

$$\Gamma = \Gamma_0 \frac{\rho_0}{\rho} \tag{2}$$

where Γ_0 is a constant characteristic of the material and ρ_0 is the initial density.

On the other hand, the momentum and energy conservation equations are:

$$\rho \frac{\partial \mathbf{v}}{\partial t} = -\nabla P + \nabla \cdot \mathbf{S} \tag{3}$$

$$\rho \frac{\partial E}{\partial t} = P \frac{1}{\rho} \frac{\partial P}{\partial t} + \mathbf{S} : \dot{\mathbf{e}} \tag{4}$$

where $\mathbf{v}$ is the velocity, $\dot{\mathbf{e}}$ is the rate of change of the deviatoric strain tensor and $\mathbf{S}$ is the deviatoric stress tensor.

The equation of state and the equation of energy conservation are coupled through the pressure and the internal energy. The Hugoniot equations relate the pressure, internal energy and density behind the shock waves to the corresponding quantities in front of them in terms of the shock velocity u_s and the particle velocity u_p. The Hugoniots of many materials can be adequately represented by the following linear relationship [25]:

$$u = c_0 + s u_p \tag{5}$$

where c_0 and s are fitting parameters that depend on the considered material and are experimentally measured.

The deviatoric part of the material is modelled by using a perfectly elastoplastic model (i.e. the yielding plastic surface does not change with the plastic deformation) with a von Mises yield surface and an associative plastic flow. This model needs two parameters, namely the shear modulus G and the yield strength Y that defines the onset of the plastic range. The algorithm to calculate the stresses checks if the material has reached the plastic regime or if it is within the elastic one. In this last case the elastic relationship is used and if plastification occurs the classical radial return algorithm [26] for the updating of stresses is applied. The magnitude that controls if an integration point has reached the plastic regime is the equivalent von Mises stress defined as:

$$\sigma_{VM} = \sqrt{\frac{3}{2} \mathbf{S} : \mathbf{S}} \tag{6}$$

The medium to be modeled is a layer of thickness d that is large compared to the wavelength λ of the perturbation imposed on the front of the layer ($kd \gg 1$, $k = 2\pi/\lambda$) in such a way that the layer can be taken as a semi-space. The amplitude of the perturbation is ξ_i. Besides, we have taken symmetry boundary conditions at the edges so that we simulate a layer of infinite lateral extent. This layer has been meshed with four-nodes plane strain elements with one integration point. The initial perturbation is needed to initialize the Richtmyer-Meshkov instability. However, to simulate planar shock wave propagation we take $\xi_i = 0$.

3. SHOCK PROPAGATION IN AN ELASTOPLASTIC SOLID

When a pressure is applied on a solid specimen a planar wave propagates into it. Following the classical elastoplastic

theory, if the stress is below the yield stress, a single elastic wave is generated. If the stress is above the yield stress two waves are generated: a plastic wave which amplitude is equal to the applied pressure and an elastic wave (called the elastic precursor) which amplitude is the Hugoniot elastic limit (HEL) [27]. Using the Mie-Gruneisen equation of state for the volumetric part and a perfectly elastoplastic constitutive law for the deviatoric part, the stress on the Hugoniot is calculated from the equation [28]:

$$\sigma_H = P_H + \frac{2}{3}Y \tag{7}$$

where P_H is obtained from the equation of state:

$$P_H = \frac{\rho_0 c_0^2 \eta}{(1 - s\eta)^2} \tag{8}$$

with the volumetric compressive strain η defined as:

$$\eta = 1 - \frac{\rho_0}{\rho} \tag{9}$$

Some simulations have been performed on flat aluminium samples of thickness $d = 80\ mm$. The material data for aluminimu are: $\rho_0 = 2700\ kg/m^3$, $c_0 = 5380\ m/s$, $s = 1.337$ and $\Gamma_0 = 2.16$. The deviatoric part is defined by means of the shear modulus $G = 40\ GPa$ and the yield strength $Y = 1\ GPa$. Three different pressures have been applied to the specimen to generate the shock waves: $P_0 = 2, 10$ and $20\ GPa$.

We are interested in the component of the stress tensor in the direction of the wave propagation σ_{11}. The stress distribution along the specimen for a time of $t = 8\ \mu s$ is shown in Fig. (**1**). The density of the material that is between both shock fronts is $\rho = 2734\ kg/m^3$, so the volumetric strain is $\eta = 0.0124$ and $P_H = 1\ GPa$ for the three applied pressures. Applying equation (7) $\sigma_H \approx 1.67\ GPa$ that coincides quite well with the amplitude of the elastic precursor obtained from the simulations ($\approx 1.7\ GPa$).

For low compressions $\eta \ll 1$ and then $\varepsilon_{11} = \ln(1 - \eta) \approx -\eta$, so the velocity of the elastic precursor is:

$$c_e = \sqrt{\frac{c_0^2}{(1 - s\eta)^2} + \frac{4G}{3\rho}} \tag{10}$$

The velocity, according this expression, is $7042\ m/s$ that is correctly predicted by the simulations ($\approx 7010\ m/s$). On the other hand, the velocity of the plastic wave depends on the applied pressure and fulfils the linear relationship $u_s = c_0 + s u_p$. The velocity of the particles obtained form the simulations are, respectively $109, 588$ and $1088\ m/s$ and

then the velocity of the plastic waves are $5525, 6166$ and $6834\ m/s$, that are correctly predicted by measuring them from the position of the shock front in Fig. (**1**) ($\approx 5620, 6200$ and $6862\ m/s$) with increasing accuracy for higher applied pressures.
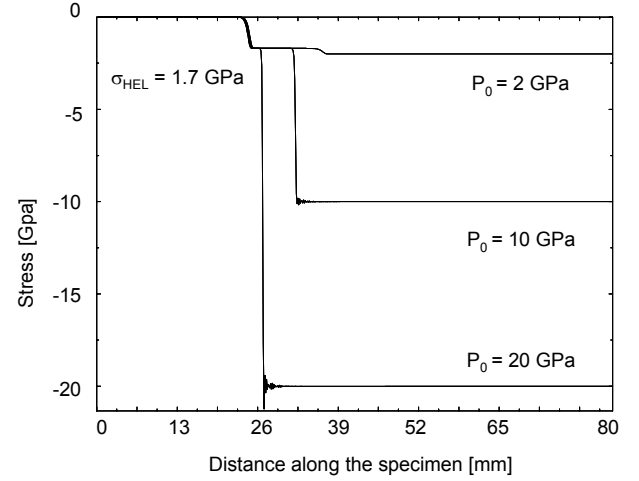
Fig. (1). Stress distribution along the specimen for the three applied pressures for a time of $t = 8\ \mu s$. The represented stress component is σ_{11} where 1 is the direction of the wave propagation.

In Fig. (**2**) the equivalent von Mises stress is represented along the specimen for a time of $t = 8\ \mu s$. It is possible to see that the zone that is plastified is the one between the two front shocks. Behind the plastic wave, the material behaves in a hydrostatic-like manner and the equivalent von Mises stress decreases when the applied pressure increases ($\sigma_{VM} = 0.54\ GPa$ for $P_0 = 10\ GPa$ and $\sigma_{VM} = 0.09\ GPa$ for $P_0 = 20\ GPa$).

So although with shock experiments is possible to determine the Hugoniot elastic limit, the stress state in the shocked state remains unknown. We explore in the next section the use of the Richtmyer-Meshkov instability to obtain the yield strength in such sock states.
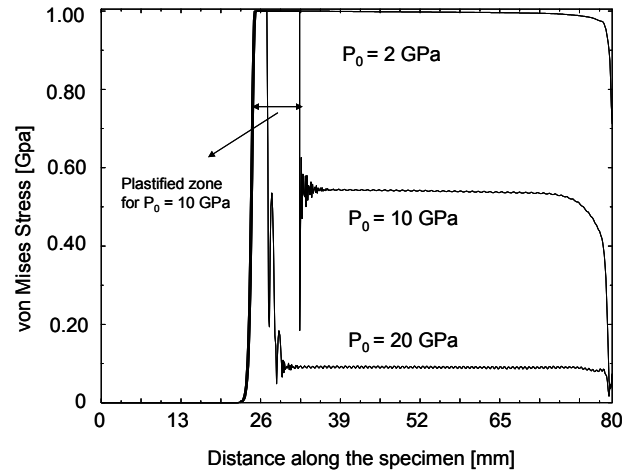
Fig. (2). Equivalent von Mises stress along the specimen for the three applied pressures for a time of $t = 8\ \mu s$.

4. EVALUATION OF THE DYNAMIC YIELD STRENGTH OF SOLIDS BY MEANS OF THE RICHTMYER-MESHKOV INSTABILITY

4.1. Description of the Richtmyer-Meshkov Instability in Solids

Classical Richtmyer-Meshkov instability (RMI) develops when a shock passes through the corrugated interface between two ideal fluids. The small perturbations of the interface between both media will grow without bound for any wavelength of the perturbation. There are very few works about RMI in solids. Plohr and Plohr [29] have presented a solution of the evolution of the interface amplitude between two elastic solids with a fixed relation between their shear moduli. These authors named RMI in elastic solids 'Richtmyer-Meshkov flow' because the presence of the elastic force always leads to a stable, oscillatory evolution of the perturbation amplitude. Their study gives the oscillation period of such an oscillatory evolution. Applying a relatively simple analytical model, we have obtained a general scale law for the period of the oscillation that has been validated with extensive two dimensional simulations for any combination of the shear moduli [30]. Also we have given an analytical model for RMI in elastoplastic solids [21] validated against extensive finite element simulations. This model is valid for any degree of compression of the media but in the case of a low compression predicts quite well the scaling law suggested for Bakharakh *et al.* [31] obtained from numerical simulations. The analytical model is the same we have used to solve the Rayleigh-Taylor in elastic solids [32,33] including the case of solids of finite thickness [34].

The main features of the RMI in solids can be seen in Figs. (**3**, **4**) where some typical responses are shown (The material and geometrical data for these calculations are given in the figures). We have applied a pressure on the free surface of an elastoplastic solid and we have represented the time history of the relative perturbation amplitude $\xi - \xi_i$. The free surface has a perturbation of the form

$$\xi(x) = \xi_i \cos\left(\frac{2\pi}{\lambda} x\right),$$ so we have defined the relative

perturbation amplitude for any time as

$$\left(\xi - \xi_i\right)(t) = \frac{u(x=0,t) - u(x=\lambda/2,t)}{2} - \xi_i$$ where u is the

nodal displacement. Obviously, for the initial time, $t = 0$, $\xi - \xi_i = 0$.

In Fig. (**3**) we can see that, for the classical case, the perturbation amplitude grows linearly as the theory predicts. On the other hand, a pure elastic material presents a stable, oscillatory pattern. Between these two extreme situations the elastoplastic cases are located. Fig. (**4**) shows that there is an initial transient phase that lasts a time t_0 during which the material behaves classically and the perturbation amplitude grows up to a value $\xi_0 > \xi_i$. The initial transient phase of the elastoplastic cases (for $t \leq t_0$) follows the classical growth,
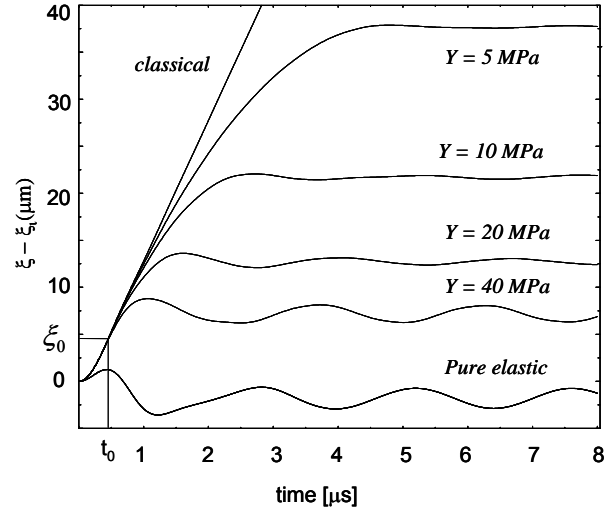
Fig. (3). Time evolution of the perturbation amplitude for different values of the yield strength Y. Applied pressure $P_0 = 10\,GPa$, wavelength and initial amplitude of the perturbation $\lambda = 5\,mm$, $\xi_i = 20\,\mu m$, shear modulus $G = 13\,GPa$, initial density $\rho_0 = 2700\,kg/m^3$, EOS parameters $c_0 = 5380\,m/s$, $s = 1.337$, $\Gamma = 2.16$.

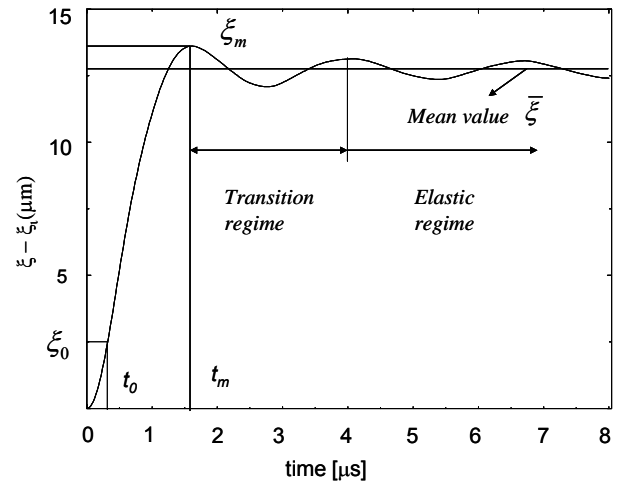**Fig. (4).** Time evolution of the perturbation amplitude for $Y = 20\,MPa$. Applied pressure $P_0 = 10\,GPa$, wavelength and initial amplitude of the perturbation $\lambda = 5\,mm$, $\xi_i = 20\,\mu m$, shear modulus $G = 13\,GPa$, initial density $\rho_0 = 2700\,kg/m^3$, EOS parameters $c_0 = 5380\,m/s$, $s = 1.337$, $\Gamma = 2.16$.

so the initial velocity $\dot{\xi}_0$ is the slope of the classical curve. After this initial transient phase the perturbation amplitude grows up to a maximum value ξ_m that essentially depends on the yield strength Y and then it remains oscillating elastically around a mean value $\overline{\xi}$. For higher values of the yield strength the maximum reached for the perturbation

amplitude ξ_m is smaller, so that in the limit $Y \to \infty$ the elastic case is recovered and for $Y \to 0$ we have the classical situation. Also it is important to note that the amplitude of the elastic oscillations is smaller for the lower values of Y. In these situations, the maximum value ξ_m and the mean value $\overline{\xi}$ are practically the same.

Our analytical model gives a scaling law for the maximum point $\left(\xi_m, t_m \right)$ reached for the perturbation amplitude and for the elastic oscillation period as well as the amplitude of such oscillation in the asymptotic elastic regime [21]. The model does not describe the initial transient phase, so it is necessary to know the values of ξ_0 and t_0 that have been evaluated from the numerical simulations. The amplitude ξ_0 is taken as the value at the time t_0 when the amplitude evolution has an inflection point. The reason of this assumption is that for $t \leq t_0$ the perturbation grows classically and then the acceleration of the amplitude perturbation is $\ddot{\xi} \geq 0$ while for $t \geq t_0$ the perturbation grows in the plastic regime and then it must be $\ddot{\xi} \leq 0$ because the plastic force is slowing down the perturbation growth. At this time, $t = t_0$ the asymptotic classical velocity $\dot{\xi}_0$ has been reached and is given by:

$$\dot{\xi}_0 = k \xi_i u_p \tag{11}$$

The scaling law we have found for the maximum amplitude is given by [21]:

$$\xi_m - \xi_0 \approx 0.29 \frac{\rho \dot{\xi}_0^2}{kY} \tag{12}$$

and if $\xi_m - \overline{\xi} << \xi_m - \xi_0$ and then $\xi_m \approx \overline{\xi}$:

$$\overline{\xi} - \xi_0 \approx 0.29 \frac{\rho \dot{\xi}_0^2}{kY} \tag{13}$$

4.2. Evaluation of the Yield Strength

In this section we show how the yield strength could be obtained form shock experiments. We are not going into the technical details of such an experiment. We are thinking in a laboratory with a facility to induce a shock wave in a solid

and with the diagnostics to measure the growth of the perturbation on the interface. Next, the procedure to obtain the yield strength from this experimental setup is described.

Suppose we want to validate the model of Steinberg *et al.* [35] which gives the value of the shear modulus G and the yield strength Y as functions of deformation ε, pressure P and temperature T. One important assumption of this model is that rate effects become insignificants for high stresses, above 10 GPa. The idea is to obtain the yield strength at different pressures by measuring the RM instability and to verify the theoretical predictions of the Steinberg model. The constitutive equations of this model are the following:

$$G = G_0 \left[1 + \left(\frac{G'_P}{G_0} \right) \frac{P}{\eta_s^{1/3}} + \left(\frac{G'_T}{G_0} \right) (T - 300) \right] \tag{14}$$

$$Y = Y_0 \left[1 + \beta \left(\varepsilon + \varepsilon_i \right) \right]^n \times \left[1 + \left(\frac{G'_P}{G_0} \right) \frac{P}{\eta_s^{1/3}} + \left(\frac{G'_T}{G_0} \right) (T - 300) \right] \tag{15}$$

subject to the limitation

$$Y_0 \left[1 + \beta \left(\varepsilon + \varepsilon_i \right) \right]^n \leq Y_{\max} \tag{16}$$

where $\eta_s = \rho / \rho_0 = 1/(1 - \eta)$, ε_i is the initial equivalent plastic strain and n and β are work-hardening parameters. In any case, to simplify the use of these equations to evaluate the yield strength in different shock states we have used the value of $Y_{\max}$ given for Steinberg for the first term of equation 16. For aluminium the data are: $G_0 = 27.6\ GPa$, $Y_{\max} = 0.68\ GPa$, $\frac{G'_P}{G_0} = 65\ TPa^{-1}$ and $-\frac{G'_T}{G_0} = 0.62\ kK^{-1}$.

The temperature in the shock state is calculated from the equation of state according to:

$$T = T_0 e^{\Gamma \eta} + \frac{s c_0^2}{C_v} e^{\Gamma \eta} \int_0^\eta e^{-\Gamma \eta} \frac{\eta^2}{(1 - s\eta)^3} d\eta \tag{17}$$

where C_v is the specific heat that for aluminium is $930\ \frac{J}{kgK}$ and the volumetric compressive strain η is obtained from equation 8

Table 1. Volumetric Compressive Strain η, Temperature T (Both Obtained from de Equation of State), Yield Strength Y and Shear Modulus G (Both Calculated from the Steinberg Model)

$P_0\ (GPa)$	10	20	30	40	50	60	70	80	90	100
η	0.08	0.15	0.20	0.24	0.26	0.28	0.30	0.32	0.34	0.35
$T\ (K)$	366	497	706	1011	1236	1524	1909	2400	3035	3420
$Y\ (GPa)$	1.08	1.43	1.74	1.99	2.28	2.54	2.75	2.90	2.99	3.20
$G\ (GPa)$	43.96	58.28	70.61	81.02	92.74	103.3	111.8	117.9	121.5	129.9

In Table **1** the values of η, T, Y and G for several applied pressures are shown. Taking into account that melting in aluminium occurs around 125 GPa for shock compression [36] we have considered a maximum value of 100 GPa.

Now, we simulate numerically some possible experiments for three different shock pressures $P_0 = 10, 40$ and $100\ GPa$. In order to do that we apply the numerical method described in section 2 with the data of Y and G obtained form Table **1**. Applying the procedure we are proposing we should recover the value of the yield strength from just one measurement of the time histories of the relative perturbation amplitude that are given in Fig. (**5**).
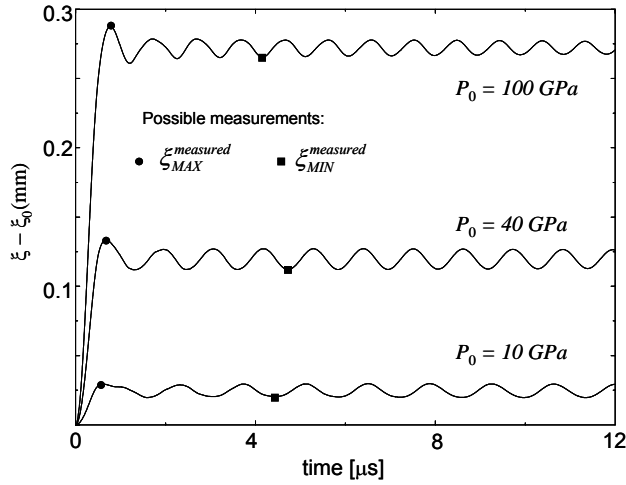
Fig. (5). Time evolution of the perturbation amplitude for three different pressures with the material data obtained from the Steinberg model.

If in a real experiment it is possible to take only one measurement, this will be between the maximum value (marked with a black circle in the figure) and the minimum one (marked with a black square). Because it is not possible to calculate ξ_0, we use an approximation of the scaling law to obtain the yield strength:

$$Y^{measured} \approx 0.29 \frac{\rho \dot{\xi}_0^2}{k \xi^{measured}} \tag{18}$$

To evaluate the rest of the terms of this equation, we need the volumetric compressive strain that is obtained from equation 8. Then, the density postshock is evaluated according to equation 9 and to calculate the asymptotic classical velocity $\dot{\xi}_0$ (equation 11) we need the particle velocity u_p that is again evaluated from the equation of state according to the expression:

$$u_p = \frac{c_0 \eta}{1 - s\eta} \tag{19}$$

The calculated values of these parameters are collected in Table **2** where the maximum and minimum measurements of the relative perturbation amplitudes are also indicated. With these data we can evaluate the yield strength Y, from the scaling law. These values are also indicated in Table **2**

For the applied pressure of 100 GPa we evaluate a yield strength between 2.7 and 3.0 GPa that gives an error within 7.5% and 13%, when comparing with the value predicted by the Steinberg model and used in the simulation of 3.2 GPa. For the pressure of 40 GPa the error is within 20% and 30% (1.4 GPa – 1.6 GPa, versus 1.99 GPa). For lower pressures the error increases, so for 10 GPa we find 0.50 GPa – 0.75 GPa, versus 1 GPa which gives an error within 25% and 50%.

Table 2. Values of the Yield Strength Y for Three Different Pressures Obtained from the Measurement of the Richtmyer-Meshkov Instability

$P_0\ (GPa)$	10	40	100
η	0.096	0.24	0.35
$\rho\ (kg/m^3)$	2986	3552	4153
$u_p\ (m/s)$	592	1901	3600
$\dot{\xi}_0\ (m/s)$	148	477	904
$\xi_{MIN}^{measured}\ (m)$	20 x 10⁻⁶	0.112 x 10⁻³	0.26 x 10⁻³
$Y_{MAX}^{measured}\ (GPa)$	0.75	1.6	3
$\xi_{MAX}^{measured}\ (m)$	30 x 10⁻⁶	0.13 x 10⁻³	0.29 x 10⁻³
$Y_{MIN}^{measured}\ (GPa)$	0.50	1.4	2.7

The method works very well for high pressures and somewhat worse for the lower ones. The reason is not in the method itself, but in the intrinsic difficulty of calculating ξ_0.

However, one interesting advantage of the proposed method is that only one experimental measurement is needed to evaluate the yield strength in opposition to the Rayleigh-Taylor based technique that needs, at least, two experimental points to calculate the growth rate. This is a very important fact because, in this kind of experiments, it is quite difficult to perform more than one measurement. The short time the experiment lasts forces to carry out two different experiments in exactly the same conditions, which is also a difficult task. However, as we have mentioned before, we do not propose to use this method instead of the Rayleigh-Taylor based technique. Both methods are complementary and they can produce useful information about the dynamic yield strength of solids in different regimes.

5. CONCLUSIONS

The knowledge of the dynamic yield strength in extreme conditions is very important in many technological applications as well as in basic science and several methods to evaluate it, have been proposed since the pioneer works of Sir GI Taylor. One of these methods is based on measuring the growth of the Rayleigh-Taylor instability and to correlate such growth with the yield strength of the material. To this end it is necessary to perform a quasi-isentropic compression of the solid that is a challenging process that needs a very big facility and so far has allowed for obtaining just one measurement in each individual experiment. So, obtaining the growth rate requires performing, at least, two different experiments in the same conditions. We propose a method based on the same philosophy but using another hydrodynamic instability, namely, the Richtmyer-Meshkov instability. To provoke this instability a shock is needed, so it is possible to use more modest facilities. Moreover and because of the time evolution of the Richtmyer-Meshkov instability in solids only one experimental measurement is necessary to evaluate the yield strength. We support the proposed technique with an analytical model that we have presented elsewhere [21] and that describes, for the first time, the evolution of the Richtmyer-Meshkov instability in elastoplastic solids. The method is valid below the melting pressure value that is about 125 GPa in Aluminium. For Iron this pressure is higher than 240 GPa [6,7] which is in the range of interest for studies related to the interior of terrestrial planets and for a heavy metal like Tantalum the melting pressure is 300 GPa [37] a value that is in the range of interest for some of the high energy density experiments planned at the Gesellschaft für Schwerionenforschung (GSI), Darmsdadt, within the framework of the new FAIR (Facility for Antiproton and Ion Research) facility [38]. The proposed method can be a valuble experimental procedure to give information about the strength of materials in shock states and, in this sense, it is complementary to the Rayleigh-Taylor technique which explores the regime of isentropic compressions.

ACKNOWLEDGEMENTS

REFERENCES

[1]   Vogler TJ, Chhabildas LC. Strength behaviour of materials at high pressures. Int J Impact Eng 2006; 33: 812-25.

[2]   Kanel GI, Razorenov SV, Baumung K, Singer J. Dynamic yield and tensile of aluminium single crystals at temperatures up to the melting point. J Appl Phys 2001; 90: 136-43.

[3]   Ocaña JL, Morales M, Molpeceres C, Torres J. Numerical simulation of surface deformation and residual stresses field in laser shock processing experiments. Appl Surf Sci 2004; 238: 242-8.

[4]   Merkel S, Wenk HR, Badro J, et al. Deformation of (Mg-0.9, Fe-0.1)SiO3 Perovskite aggregates up to 32 GPa. Earth Planet Sci Lett 2003; 209: 351-60.

[5]   Boehler R. High-pressure experiments and the phase diagram of lower mantle and core materials. Rev Geophys 2000; 38: 221-45.

[6]   Willians Q, Jeanloz R, Bass J, Svendsens V, Ahrens TJ. The melting curve of iron to 250 GPa: A constraint on the temperature at Earth's center. Science 1987; 236: 181-2.

[7]   Laio A, Bertrand S, Chiarotti GL, Scandolo S, Tossati E. Physics of iron at Earth's core conditions. Science 2000; 287: 1027-30.

[8]   Taylor GI. The use of flat-ended projectiles for determining dynamic yield stress. I. Theoretical considerations. Proc R Soc A 1948; 194: 289-99.

[9]   Whiffin AC. The use of flat-ended projectiles for determining dynamic yield stress. II. Tests on various metallic materials. Proc R Soc A 1948; 194: 300-22.

[10]   Wilkins ML, Guinan MW. Impact of cylinders on a rigid boundary J Appl Phys 1973; 44; 1200-6.

[11]   Zukas JA. Introduction to hydrocodes (Studies in Applied Mechanics 49). Amsterdam: Elsevier 2004.

[12]   Barnes JF, Blewett PJ, McQueen RG, Meyer KA, Venable D. Taylor instability in solids. J Appl Phys 1974; 45: 727-32.

[13]   Barnes JF, Janney DH, London RK, Kenneth AM, Sharp DH. Further experimentation on Taylor instability in solids. J Appl Phys 1980; 51: 4678-9.

[14]   Kalantar DH, Remington BA, Colvin JD, et al. Solid-state experiments at high pressure and strain rate. Phys Plasmas 2007; 7: 1999-2006.

[15]   Colvin JD, Legrand M, Remington BA, Schurtz G, Weber SV. A model for instability growth in accelerated solid metals. J Appl Phys 2003; 93: 5287-301.

[16]   Edwards J, Lorenz KT, Remington BA, et al. Laser-driven plasma for shockless compression and acceleration of samples in the solid state. Phys Rev Lett 2004; 92: 075002.

[17]   Lorenz KT, Edwards MJ, Glendinning SG, et al. Accesing ultrahigh-pressure, quasi-isentropic states of matter. Phys Plasmas 2005; 12: 056309.

[18]   Lorenz KT, Edwards MJ, Jankowski AF, Pollaine SM, Smith RF, Remington BA. High pressure, quasi-isentropic compression experiments on the Omega laser. High Energy Density Phys 2006; 2: 113-25.

[19]   Remington BA, Allen P, Bringa EM, et al. Material dynamics under extreme conditions of pressure and strain rate. Mater Sci Technol 2006; 22: 474-88.

[20]   Mikhailov AL. Hydrodynamic instabilities in solid media. From the object of investigation to the investigation tool. Phys Mesomechan 2007; 10: 265-74.

[21]   Piriz AR, López Cela JJ, Tahir NA, Hoffmann DHH. Richtmyer-Meshkov instability in elastic-plastic media. Phys Rev E 2008; 78(5): 056401.

[22]   Kerley GI. Theoretical equation of state for aluminium. Int J Impact Eng 1987; 5: 441-449.

[23]   ABAQUS Finite Element Code, Version 6.7. Hibbit, Karlson and Sorensen Inc. Pawtucket, RI 2007.

[24]   Swegle JW, Robinson AC. Acceleration instability in elastic-plastic solids I. Numerical simulations of plate acceleration. J Appl Phys 1989; 66(7): 2838-58.

[25]   McQueen RG, Marsh SO, Taylor JW, Fritz JN, Carter WJ. The equation of state of solids from shock wave studies. In: Kinslow R, Ed. High-velocity impact phenomena, New York, Academic Press 1970; pp. 293-417.

[26]   Hughes TJR. Numerical implementation of constitutive models: rate independent deviatoric plasticity. In Asaro R, Nemat-Nasser S, Hegemier G, Ed. Theoretical Foundations for Large Scale Computations of Nonlinear Material Behavior, The Netherlands, Martinus Nijhoff Publishers 1984; pp. 29-57.

[27]   Davison L. Fundamentals of shock wave propagation in solids (Shock wave and high pressure phenomena). Berlin Heidelberg: Springer-Verlag 2008.

[28]   Steinberg DJ, Sharp RW. Interpretation of shock-wave data for beryllium and uranium with an elastic-viscoplastic constitutive model. J Appl Phys 1981; 52(8): 5072-83.

[29]   Plohr JN, Plohr BJ. Linearized analysis of Richtmyer-Mehkov flow for elastic materials. J Fluid Mech 2005; 537: 55-89.

[30]   Piriz AR, López Cela JJ, Tahir NA, Hoffmann DHH. Richtmyer-Meshkov flow in elastic solids. Phys Rev E 2006; 74: 037301.

[31]   Bakhrakh SM, Drennov OB, Kovalev NP, *et al*. Hydrodynamic instability in strong media. Report No. UCRL-CR-126710, Lawrence Livermore National Laboratory, Livermore, California 1997 (unpublished).

[32]   Piriz AR, López Cela JJ, Cortázar OD, Tahir NA, Hoffmann DHH. Rayleigh-Taylor instability in elastic solids. Phys Rev E 2005; 72: 056313.

[33]   López Cela JJ, Piriz AR, Serna Moreno MC, Tahir NA. Numerical simulations of Rayleigh-Taylor instability in elastic solids. Laser Part Beams 2006; 24: 427-35.

[34]   Piriz AR, López Cela JJ, Serna Moreno MC, Tahir NA, Hoffmann DHH. Thin plate effects in the Rayleigh-Taylor instability of elastic solids. Laser Part Beams 2006; 24: 275-82.

[35]   Steinberg DJ, Cochran SG, Guinan MW. A constitutive model for metals applicable at high-strain rate. J Appl Phys 1980; 51: 1498-504.

[36]   Furnish MD, Chhabildas LC, Reinhart WD. Time-resolved particle velocity measurements at impact velocities of 10 km/s. Int J Impact Eng 1999; 23: 261-70.

[37]   Luo SN, Swift DC. On high-pressure melting of tantalum. Phys Rev Condens Matter 2007; 388: 139-44.

[38]   Tahir NA, Deutsch C, Fortov VE, *et al*. Proposal for the study of thermophysical properties of high-energy-density matter using current and future heavy-ion accelerator facilities at GSI Darmstadt. Phys Rev Lett 2005; 95: 035001.